CONF-960949--3

A NEW CONCEPT POSITIVE (NEGATIVE) SURFACE IONIZATION SOURCE FOR RIB APPLICATIONS

G. D. Alton[1], R. F. Welton[2], B. Cui[3], S. N. Murray, and G. D. Mills
Oak Ridge National Laboratory, P. O. Box 2008,*
Oak Ridge, Tennessee 37831-6368

Abstract

A versatile, new concept, spherical-geometry, positive (negative) surface-ionization source has been designed, fabricated, and initial tests completed which can operate in either positive- or negative-ion beam generation modes without mechanical changes to the source. The highly permeable, composite Ir/C has an intrinsic work function of $\phi = 5.29$ eV and can be used directly for the generation of positive-ion beams of highly electropositive elements. For negative-surface ionization, the work function is lowered by dynamic flow of a highly electropositive adsorbate such as Cs through the ionizer matrix. The results of initial testing indicate that the source is reliable, stable and easy to operate, with efficiencies for Cs^+ estimated to exceed 60% and as high as ~ 50% for F^- generation. The design features, operational principles, and initial performance of the source for generating Cs^+ and F^-, when operated with Cs, are discussed in this article.

PACS:
Keywords: Ion source, surface ionization, negative surface ionization, positive surface ionization.

[1] Corresponding author. Address: Oak Ridge National Laboratory, P. O. Box 2008, Oak Ridge, TN 37831-6368 USA. Telephone: 423-574-4751, FAX: 423-574-1268, E-mail: gda@mail.phy.ornl.gov.
[2] Oak Ridge Institute of Science and Engineering (ORISE), Oak Ridge, TN
[3] China Institute of Atomic Energy (CIAE), Beijing, China.
* Managed by Lockheed Martin Energy Research Corp. under contract No. DE-AC05-96OR22464 with the U.S. Department of Energy.

1.0 Introduction

Ion sources based on the surface-ionization principle are generally characterized by a high degree of ion beam purity, low energy spread, and limited range of species capability. The ionization efficiency can be very high or low, depending on the electrochemical character of the species in relation to the work function of the ionizing surface. The energy spread of the ion beam is characteristically very low and is of the order of thermal energies ~ 2kT (<< 1 eV). Surface ionization sources can be described according to the means by which the atomic or molecular vapor is fed onto the ionizing surface and the method used to extract the ions. Ionization can be effected by impinging vapor onto a hot metal surface or allowing the vapor to diffuse through a porous matrix. For efficient positive ionization, the work function of the metal must be high and several metals may be chosen for this application.

Positive surface ionization has been utilized for a number of applications, including: sputter-type negative-ion sources, enhancing negative-ion yields for secondary ion mass spectrometry (SIMS) applications, microfocused ion beam applications, and space-craft propulsion. Several examples of this type of source are described in Ref. 1. The surface-ionization process is also highly chemically selective and, therefore, can be used to great advantage for radioactive ion beam (RIB) applications where isobaric contamination problems may be important. Therefore, the surface ionization source has also been utilized to generate low-energy positive RIB beams at ISOL facilities (see, e.g., Refs. 2-4).

In contrast to positive surface ionization, the work function must be low for efficient negative surface ionization. Negative surface ionization has not been utilized frequently as a means for production of ion beams – principally due to the lack of chemically stable low-work-function materials for use as ionizers. LaB_6 is the most frequently used low-work-function surface ionizer, having a work function ranging between 2.3 and 3.2 eV [5–9]. A few sources based on the use of LaB_6 ionizers have been described in the literature (see for example, Refs. 10–12). Unfortunately, LaB_6 is easily poisoned [13] which affects the reliability of operation of sources equipped with this material [11]. Despite this problem, LaB_6 has also been used at ISOL facilities for negative-ion generation of high-electron-affinity radioactive species with some success (see for example, Refs. 2 and 12). In principle, the negative surface complement of the ionization source described in this report, overcomes the handicap of being easily poisoned because of the continuously renewable supply of a work-function-lowering agent.

2.0 Ion Source design

The design features of the positive (negative) surface ionization source under evaluation for potential use at the HRIBF [14] are schematically illustrated in Fig. 1. The source is intended to be used as a complementary replacement for the electron impact ionization sources presently in use at the HRIBF [15,16] for pending RIB generation and, therefore, is designed to mount in the same vacuum envelope. For RIB generation, collimated ^1H, ^2D, ^3He, and ^4He ion beams from the Oak Ridge Isochronous Cyclotron (ORIC) will pass through a thin window in the target material reservoir where they will interact with the refractory target materials chosen for the production of the desired radioactive beam. The species of interest are diffused from the target material which is maintained at high temperature during the production process. The target material reservoir is positioned within the inner diameter of a series-connected, resistively-heated, Ta tube designed to reach temperatures exceeding 2000°C. The power required to heat the target reservoir assembly to this temperature is ~ 2.25 kW (4.5 V at 500 A). The ionizer and vapor transport tube are heated resistively to ~ 1100°C–1450°C, depending on the critical temperature required to evaporate the species of interest in ionic form, by passing a current through the tubular structure. The source can

be used directly as a positive surface ionization source. Ionization occurs as the particles are evaporated from the surface of the highly permeable, spherical-geometry ionizer. The cathode (anode) assembly electrode structure is insulated from the source housing so that a (positive) negative potential up to ± 1 kV can be applied for initial acceleration of ions formed on the hot ionizer surface. The electrode structure is designed to focus the ion beam through the ion exit aperture of the cathode(anode), where it is further accelerated to energies between ~ 20 keV and 50 keV.

When operated in the negative-surface-ionization mode, the work function is lowered to some nominal value by feeding a highly electropositive vapor through the permeable matrix. Conversion to the negative mode is made by applying power to an external oven containing the work function lowering agent. In principle, this technique can be utilized for the efficient generation of negative-ion beams from high-electron-affinity elements such as members of the group VIIA elements (F, Cl, Br, I, At) and, perhaps, other members of the periodic chart, either in atomic or molecular form. Several, penta and hexafluoride molecules, have high electron affinities (e.g., E_A (MoF_5) = 3.3 eV; E_A(MoF_6) = 4.5 eV; E_A (SeF_6) = 3.0 eV; E_A (TeF_6) = 3.34 eV; E_A(ReF_6) = 3.9 eV; E_A (IrF_6) = 4.3 eV; E_A (WF_6) = 4.3 eV; E_A(UF_5) = 4.0 eV; and E_A (UF_6) = 5.1 eV). The group VIIA elements (halogens) all have high electron affinities (E_A (F) = 3.4 eV; E_A (Cl) = 3.6 eV; E_A (Br) = 3.66 eV; E_A (I) = 3.076 eV). These atomic and molecular species, as well as an extended list of other species, are candidates for ion beam formation though negative surface ionization, provided that the dynamic flow technique is effective in producing a chemically stable, low-work-function surface and does not introduce other problems associated with the negative ion beam generation process.

For optimum efficiencies, the adsorbate should be fed at a rate commensurate with maintaining ~ 0.5 monolayer of adsorbate on the surface (~ 1.3×10^{14} atoms/cm^2). Ideally, the electropositive species that is fed through the matrix should have a critical temperature that is higher than that of the negative species in question. This would appear to be the case for evaporation of Cs^+ and F^- from a hot Ir surface where the respective critical temperatures are found to be ~ 1450°C and ~ 1350°C.

Ionizer design. The spherical geometry ionizer (spherical radius: 2.5 mm; diameter: 6.25 mm) is machined from a highly permeable, carbon-bonded-carbon-fiber (CBCF) matrix (fiber diameter: ~ 6 μm; density ~ 0.125 g/cm^3) and then coated with ~ 5 μm of Ir by use of the chemical vapor deposition technique (CVD) [17]. Since Ir has an intrinsically high work function (ϕ = 5.29 eV), it is very efficient for positive surface ionization of the group IA members of the periodic chart (Li, Na, K, Rb, Cs, and Fr) and group IIA elements at lower efficiencies. Figure 3 displays a magnified section of the ionizer taken with a scanning electron microscope (SEM). Because of the high permeability of the CBCF structure, the species of interest, can quickly diffuse through the ionizer matrix. Surface ionization occurs as the particles are evaporated from the high work function surface.

Ion Optics. The maximum ion beam intensity I_c that can be extracted from the source for a species of mass M is governed by the space-charge-limited Child-Compton relation [18] for flow between two closely-spaced concentric spheres maintained at a potential difference of V given by

$$I_c = \frac{16\pi}{9}(2n)^{1/2}\frac{\varepsilon_0 V^{3/2}}{\alpha^2} = I_c = P_c V^{3/2} \qquad (1)$$

where $\eta = e/M$ is the ratio of the electronic charge e to the mass of the species, ε_0 is the permitivity of free space and α is dimensionless parameter given by $\alpha = \mu - 0.3\mu^2 + 0.075\mu^3 + \ldots$ and $\mu = \log r/r_c$. Values for α are tabulated in a variety of references including Ref. 19. In Eq. 1, P_c is the perveance of the electrode system where the ions are formed and receive their initial acceleration. The positive and negative ion optics of the ionizer electrode system for space-charge-limited operation of either source type are essentially identical. The ion optics of the system were initially designed by use of the code described in Ref. 20. The trajectories and equipotentials, for a 20 keV space charge limited beam of Cs^+, are displayed in Fig. 3. The perveance P_c for Cs^+ beams is found to be 8×10^{-10} [$A/V^{3/2}$] while for the lighter F^- beam, the perveance P_c is 21×10^{-10} [$A/V^{3/2}$]. However, for use in RIB applications the extracted currents will be very low and the concepts of perveance and space-charge- limited flow have no importance.

3.0 Theory of positive ion formation

Whenever an atom or molecule is near to or adsorbed on a hot metal surface, the valence band is broadened. If the level is broadened to the extent that it overlaps the Fermi level of the metal, electrons can move from the atom or molecule to the metal or from the metal to the atom or molecule, depending on the electropositive/electronegative character of the atom or molecule in relation to the work function of the metal surface. Thus, atoms or molecules may be emitted from the surface as neutral atoms or molecules or in ionic form. The process whereby ions are formed is referred to as surface ionization and obeys the appropriate positive or negative form of the Langmuir-Saha equation. In principle, the technique can be used effectively to produce either positive- or negative-ion beams from certain members of the periodic chart.

For thermodynamic equilibrium processes, the ratio of ions to neutrals that leave an ideal surface can be predicted from Langmuir-Saha surface ionization theory. For atoms or molecules with first ionization potential I_p, leaving a hot surface at temperature T and work function ϕ, the probability of positive ion formation P_i is given by

$$P_i = \frac{\omega_+}{\omega_0}\left(\frac{1-r_+}{1-r_0}\right)\exp\left(\frac{\phi - I_p}{kT}\right) \times \left[1 + \frac{\omega_+}{\omega_0}\left(\frac{1-r_+}{1-r_0}\right)\exp\left(\frac{\phi - I_p}{kT}\right)\right]^{-1} \qquad (2)$$

where r_+ and r_0 are the reflection coefficients of the positive and neutral particles at the surface, ω_+ and ω_0 are statistical weighting factors, and k is Boltzmann's constant. ω_+ and ω_0 are related to the total electronic spin S of the respective species given by

$$\omega = 2S + 1 = 2\sum_i s_i + 1,$$

where s_i is the spin on the i^{th} electron. Optimum ionization efficiencies are obtained for high-work-function materials and low-ionization-potential I_p atomic species. For elements for which $I_p > \phi$, the process is much less efficient. For example, the work function for clean tungsten is about 4.6 eV and the ionization potential for indium is 5.8 eV. Thus, in this case, the exponential term (ϕ–I_p) in the Langmuir-Saha relation is negative and, therefore, the probability of ionization

is low. The efficiency is relatively high for group IA elements, but low (10^{-2} or 10^{-3}) for elements such as In, Ca, Al, Ga, and Tl. The incident particles which are not ionized are evaporated as neutral atoms. Surface ionization sources can be highly element selective due to the fact that neighboring elements often have very different ionization potentials or electron affinities. Equation 1 applies to an idealized situation in which the surface properties are isotropic and there are no surface contaminants. The work function ϕ varies with crystalline orientation, and the presence of minute amounts of certain contaminant materials on the surface can significantly alter the local work function.

4.0 Theory of negative surface ionization

Analogously to the case for positive surface ionization, atoms or molecules can also be formed as negative ions through surface ionization. The probability P_i for leaving a metal surface as a negative ion or neutral particle depends on the magnitude of the difference between the electron affinity E_A and the surface work function ϕ of the atom or molecule, i.e., $(E_A - \phi)$. For thermodynamic equilibrium processes, the ratio of ions to neutrals which leave an ideal surface can be predicted from Langmuir-Saha surface ionization theory appropriate for negative-ion formation. The form of the Langmuir-Saha equation for the probability of negative-ion formation of neutral particles of electron affinity E_A interacting with a hot metal surface at temperature T and low work function ϕ is given by

$$P_i = \frac{\omega_-}{\omega_0}\left(\frac{1-r_-}{1-r_0}\right)\exp\left(\frac{E_A-\phi}{kT}\right)x\left[1+\frac{\omega_-}{\omega_0}\left(\frac{1-r_-}{1-r_0}\right)\exp\left(\frac{E_A-\phi}{kT}\right)\right]^{-1}. \qquad (3)$$

where r_- and r_0 are the reflection coefficients of the particle at the surface, and ω_- and ω_0 are statistical weighting factors for the negative ion and neutral atom, respectively. ω_- and ω_0 are again related to the total spin S of the respective species given by

$$\omega = 2S + 1 = 2\sum_i s_i + 1,$$

where s_i is the spin on the i^{th} electron. From Eq. 3, it is evident that negative-ion yields can be enhanced by lowering the work function ϕ or increasing the surface temperature T for elements where $E_A \leq \phi$. The former can be effected by surface adsorption of minute amounts of low-work-function materials such as the group IA and IIA elements. Analogously, the adsorption of minute amounts of highly electronegative atoms or molecules such as oxygen or the halogens can deleteriously affect the negative-surface ionization efficiency by raising the work function.

5.0 Electropositive adsorbate-induced work function changes

It is well known that atomic adsorption of a dissimilar element on a clean surface affects the surface work function. The magnitude and sign of the change depends on the chemical properties of the adsorbed atom (adsorbate) and those of the host material (adsorbent). Electropositive atoms decrease the work function while electronegative atoms tend to increase the work function. These

phenomena are exploited in SIMS as a means for enhancing both positive and negative secondary ion yields.

Semiempirical relations have been developed which relate the work function change $\Delta\phi$ to the surface coverage θ [21]. These relations can be used to predict, with good accuracy, the value of the work function ϕ over the complete range of adsorbate coverage ($\theta = 0$ to $\theta = 1$). The equation which expresses the functional dependence of ϕ on θ can be written as follows:

$$\phi(\theta) \approx \phi_0 + \frac{6\Delta\phi_m}{(3-\theta_m)\theta_m}\theta - \frac{3\Delta\phi_m(\theta_m+1)}{(3-\theta_m)\theta_m^2}\theta^2 + \frac{2\Delta\phi_m}{(3-\theta_m)\theta_m^2}\theta^3 [eV] \tag{4}$$

where ϕ_0 is the intrinsic work function of the sample and $\Delta\phi_m$ is the maximum change in surface work function induced by the adsorbate at optimum coverage θ_m. Figure 4 displays work-function ϕ versus θ for Cs vapor impinging on an Ir surface. As noted, the work function reaches a minimum value of $\phi = 1.43$ eV at $\theta = 0.5$. At $\theta = 1$, the work function approaches that of the intrinsic work function of Cs metal ($\phi = 2.18$ eV).

The change in work function at low adsorbate coverages can also be approximated as a binomial series expansion given by

$$\Delta\phi(\theta) = 3\Delta\phi_m \sum_{n=0}^{\infty} (-2)^n (\theta/\theta_m)^{(3n+2)/2} V \ , \tag{5}$$

which is valid in the region $0 \le \theta \le 0.63\theta_m$ [21].

The approximate relation for computing maximum work function changes $\Delta\phi_m$ that occur at optimum fractional coverages θ_m is given by

$$\Delta\phi_m \cong -1.24\left[\phi_0 - \frac{1}{2}(I_A + E_A)\right]V \tag{6}$$

where ϕ_0 is the intrinsic work function of the surface before the adsorbate is added and I_A and E_A are, respectively, the first ionization potential and electron affinity of the adsorbate material. The empirical relation is found to reproduce, with good accuracy, maximum work function changes for alkali metal and alkaline earth metal adsorption. From this expression, we note that for maximum changes in work function $\Delta\phi_m$, the term $1/2(I_A + E_A)$ should be small. Thus, the choice of adsorbate material is extremely important. Of the stable elements readily available, Cs is the most effective element in the periodic chart for this application. The expression is valid for single crystalline as well as polycrystalline materials. More details on the model and the accuracy of Eq. 6 for predicting maximum work functions for a number of adsorbate/adsorbent combinations are given in Ref. 21. Table I lists a few low work function surfaces, some of which are induced to low values by adsorption of a fractional monolayer of a highly electropositive adsorbate material while others are alloys or mixes of materials.

6.0 Adsorption/Evaporation

The Cs^+ beam intensity is governed by the rate at which Cs atoms strike the ionizer surface and the rate at which the ions leave the ionizer surface through evaporation. The rate of neutrals arriving at the ionizer surface is governed by the vapor pressure of cesium in the reservoir, the conductance of the vapor transport tube, and the temperature of the system. As the Cs oven temperature is increased, more cesium vapor flows into the source body. This rise in absolute cesium pressure causes more cesium to strike the surface of the ionizer, resulting in higher beam currents. The number of neutral particles dN/dt striking the ionizer per unit area per unit time is given by the familiar relation

$$dN/dt = n_0\bar{v}/4 = \frac{n_0}{4}\left(\frac{8}{\pi}\frac{kT}{M}\right)^{1/2} \tag{7}$$

where $\bar{v}$ is the average velocity of a cesium atom of mass M within the ionizer/transport tube chamber at temperature T, n_0 is the number of particles per unit volume within the chamber, and k is Boltzmann's constant. The residence times t for Cs on Ir at 1450°C and 1350°C, estimated from the Frenkel relation,

$$\tau = \tau_0 e^{H_{ad}/kT} \tag{8}$$

are 220 μs and 865 μs, respectively, (heat of adsorption H_{ad} = 3.3 eV [22]; $\tau_0 = 5 \times 10^{-14}$ s). Analogously, the residence times for F on an Ir surface at the same temperatures are τ = 65 μs and 301 μs, respectively, where τ_0 is assumed to be $\tau_0 = 1 \times 10^{-15}$ s and H_{ad} is estimated to be 3.7 eV.

The arrival rate of adsorbate particles per unit area dN/dt on a surface at temperature T is given by Eq. 7. The rate of evaporation of particles from the surface per unit area $\frac{dN}{dt}$ can be expressed as

$$\begin{aligned}\frac{dN}{dt} &= NS(T)\frac{Z}{Z_{ad}Z_{vib}}\left(e^{-H_{ad}/kT}\right)N \\ &= NS(T)\frac{kT}{h}\frac{n_0}{4}\left(\frac{8kT}{\pi M}\right)^{1/2} e^{(\Delta ST - H_{ad})/kT}\end{aligned} \tag{9}$$

where S(T) is the probability of sticking to the surface, Z, Z_{ad} and Z_{vib} are respectively, the partition functions for the particle in the vacuum, following adsorption and vibrational state, ΔS is the change in entropy of the particle from the gas phase to the adsorbed state on the Ir surface. N is the number of adsorbate atoms/per unit area, k is Boltzmann's constant, and H_{ad} is the enthalpy of adsorption for the adsorbate/adsorbent combination. In steady state, the rates of arrival and evaporation are just balanced. Equating Eqs. 7 and 9 and solving for N, we arrive at an expression for the coverage N versus surface temperature given by

$$N = \frac{n_0}{4}\left(\frac{8kT}{M}\right)^{1/2} \frac{h}{S(T)kT} e^{(H_{ad}-\Delta ST)/kT} \tag{10}$$

On a relative coverage basis, we define $\theta = N/N_{max}$ where N_{max} is the adsorbate coverage where all the available adsorbent sites are filled, corresponding to a coverage of $\theta = 1$. The work function is typically minimized when $\theta_m = 0.5$. Substituting for θ, we have

$$\theta = \frac{n_0}{4}\left(\frac{8kT}{\pi M}\right)^{1/2} \frac{h}{S(T)N_{max}kT} e^{(H_{ad}-\Delta ST)/kT} \tag{11}$$

In this form, we can use Eq. 4 to estimate the work function change induced by the adsorbate coverage, θ.

For purposes of illustrating the behavior of the coverage θ versus temperature T, we apply Eq. (11) to the case of Cs vapor impinging on a hot Ir surface. We assume that the upper pressure p at which a typical electron impact ionization source can operate without compromising the ionization efficiency of the source is $p = 2 \times 10^{-4}$ Torr, the Cs atoms stick with unit probability , i.e., S(T) =1, $H_{ad} = 3.3$ eV, and that $N_{max} = 2.5 \times 10^{14}/cm^2$. In Eq. (11), we take the product of the change in entropy and temperature T, ΔST, to be –0.40 eV. Figure 5 illustrates how the relative coverage, θ, depends on the temperature of the sample surface, assuming that $\theta_m = 0.5$ at 1350°C.

7.0 Source performance: Positive ionization mode

The source (Fig. 1) was characterized in the positive surface ionization mode by feeding Cs vapor from an external oven into the vapor transport tube of the source. The tube and ionizer assembly were maintained at ~ 1450°C throughout the characterization studies for Cs^+ generation. The principal objectives of these studies were to carefully characterize the source performance in terms of intensity capability, ionization efficiency and reliability for potential use as an on-line RIB source at the HRIBF. Operational parameters, essential for efficient operation of the source as a positive surface ionizer, were derived from these studies. The parameters include: the dependence of ion beam intensity on cesium oven temperature, on ionizer temperature, and on extraction voltage. The dependencies of Cs^+ beam intensity on Cs oven temperature and on ionizer temperature are displayed, respectively, in Figs. 6 and 7. As noted, the Cs^+ beam intensity versus Cs oven temperature exhibits a characteristic maximum at ~ 200°C. In order for cesium to be thermally evaporated as ions from the surface, enough energy must be supplied to the ion to overcome the heat of adsorption H_{ad}. This energy is governed by the temperature of the ionizing surface. For Cs on Ir, H_{ad} has the value of 3.3 eV [22]. As noted in Fig. 7, the optimum Cs^+ ion beam intensity versus ionizer temperature exhibits a maximum value, or critical temperature at ~ 1450°C for Cs^+ ion evaporation and increases rather sharply when the critical temperature is reached (~ 1450°C).

Flow rate of Cs from the reservoir to the ionizer. The flow rate *dN/dt* of Cs vapor through a transport tube of length ℓ and radius a at temperature T can be calculated from the modified Poiseuille flow equation (see, for example, Ref. 23) given by

$$dN/dt = \frac{\pi a^4 \bar{p} \Delta p}{8NkT\ell} + \frac{\pi a^3 \Delta p}{M\bar{v}\ell} \qquad (12)$$

where $\bar{p} = (p_f + p_b)/2$ is the average pressure across the tube of length ℓ and $\Delta p = p_f - p_b$, the difference in pressures in the Cs reservoir p_f and in the ionizer region of the ion source p_b; $\bar{v}$ is the average velocity of a Cs atom of mass M in the transport tube given by Eq. 7.

(The length of the transport tube ℓ used during operation of the source was ℓ = 43.6 cm and the effective radius a of the tube was a = 0.0534 cm.)

We estimate the vapor pressure of Cs in the reservoir from a modified form of the Clausius-Clapeyron equation which relates the vapor pressure of Cs and temperature T of the reservoir [24] through the relation

$$p(Torr) = 8.58 \times 10^{10} \cdot T^{-1.35} \cdot 10^{-1041/T}. \qquad (13)$$

Vapor pressures calculated from this relation agree quite closely to computations determined by use of codes such as Thermo-Calc [25].

The flow rates of Cs into the ion source at the corresponding reservoir temperatures are, respectively, 4.57×10^{13} atoms/s (7.3 μA) at 185°C; 5.53×10^{13} atoms/s (8.8 μA) at 190°C; 6.08×10^{13} atoms/s (9.7 μA) at 195°C; 8.33×10^{13} atoms/s (13.3 μA) at 200°C; 1.01×10^{14} atoms/s (16 μA) at 205°C; and 1.83×10^{14} atoms/s (29.4 μA) at 210°C, as calculated by use of Eq. 12. (The equivalent Cs ion currents are also shown in parentheses.)

Cs^+ ionization efficiency estimates. If the supply rate of Cs through the Ir ionizer is greater than the rate of extraction of ions from the source, the influence of space charge will reduce the ionization efficiency of the source. Whenever the extraction potential is increased, then the ion current versus extraction voltage deviates from the space charge limited flow regime and finally reaches a saturation value where the particles are extracted as fast as they are formed. This region is termed the temperature limited regime. The intermediate region between the space charge and temperature limited ion current regimes is referred to as the transition region. These regions can be easily distinguished in Fig. 8 from the low intensity curve. The saturation current, corresponding to a Cs oven temperature of 180°C and an extraction voltage of ~ 600 V is 3.2 μA, while that for a Cs oven temperature of ~ 200°C and an extraction voltage of ~ 1000V, is ~18 μA. At saturation, there is a balance between the rate of arrival of Cs vapor at the exit side of the ionizer and ion extraction. By comparing the calculated Cs flow rates derived from Eq. (12) with the saturation currents shown in Fig. 8, assuming no extraction or beam transport losses, the estimated ionization efficiencies for the two cases are respectively, 43.8% and 61.2% for Cs^+ formation. However, if we assume that 100% of the incident flux of neutral Cs atoms stick to the surface and there are no straight-through loss channels, then all particles will be ionized at saturation.

8.0 Source performance: negative surface ionization mode

When operated in the negative-surface-ionization mode, the work function is lowered to some nominal value by feeding a highly electropositive vapor through the highly permeable matrix.

Conversion to the negative mode is made by applying power to an external oven containing the work function lowering agent (in this case Cs). In principle, this technique can be utilized for the efficient generation of negative-ion beams from high-electron-affinity elements such as members of the group VIIA elements (F, Cl, Br, I, At) and, perhaps, other members of the periodic chart, either in atomic or molecular form. For optimum efficiencies, the adsorbate should be fed at a rate commensurate with maintaining ~ 0.5 monolayer of adsorbate on the surface (~ 1.3×10^{14} atoms/cm^2). In order to be an efficient negative ion generator, the electropositive species that is fed through the matrix must have a higher critical temperature than that of the negative species in question. This would appear to be the case for Cs^+ and F^- as suggested by the data derived from these studies. Cs was chosen for lowering the work function because of its availability and ease of use in the existing source structure. Other materials such as Ba, Eu, or Ce could also be used for the same purpose; these particular materials are expected to have higher critical temperatures than Cs^+ for evaporation in ionic form. However, these elements will require more power to vaporize and transport to the ionizer surface and be less efficient in terms of their theoretical work function lowering capabilities.

Operational parameters, analogous to those for the positive surface ionization mode, were also determined for the negative surface ionization mode. The complementary operational parameter data derived from these studies which are critically important for operation of the source at optimum conditions are the dependence of F^- beam intensity on Cs oven temperature, ionizer temperature, target temperature and extraction voltage as displayed in Figs. 9, 10, 11, and 12. From the data shown in Fig. 9, we observe that the F^- beam intensity rises with Cs oven temperature in accord with that found for Cs^+ which characteristically is found to have a maximum at a temperature of 195–200°C. The critical temperature for F^- evaporation was found to be 1350°C. The ionizer was operated at this temperature throughout the F^- characterization studies. As noted, in Fig. 10, the F^- beam intensity versus ionizer temperature saturates at ~ 1350°C; this data serves as the basis of the choice for operating the ionizer during the F^- measurements and provides evidence that the critical temperature for F^- (1350°C) is lower than that for Cs^+ (1450°C), a necessary condition for the negative surface ionization mode to be a viable means for efficient generation of negative ion beams. The data shown in Figs. 11 and 12 indicate that the F^- negative ion yields can be improved by increasing the target temperature (AlF_3 vapor pressure) and extracting the ion beam at higher voltages. In the present experiments, the extraction voltages were limited to values ≤ 300 V. A typical F^- mass spectrum is shown in Fig. 13. As noted, the mass spectrum is very clean as is characteristic of the selective nature of the surface ionization process.

F^- ionization efficiency estimates. The AlF_3 was placed in the target material reservoir of the source and heated to ~ 500°C where a small fraction of the material was vaporized (vapor pressure of the AlF_3: ~ 2×10^{-7} Torr) and transported to the ionizer. Assuming no other vapor transport mechanism, the thermally dissociated AlF component of the AlF_3 is the source of atomic F for surface ionization. Thermodynamic equilibrium calculations predict that only 2.4% of the AlF vapor that is transported to the ionizer surface at a temperature of 1350°C and a partial pressure of $p = 2 \times 10^{-4}$ Torr will be dissociated [25]; this correlates to a flow rate of ~ 1.04×10^{10} F atoms/s. Since an ion current of ~ 30 nA of F^- or 1.88×10^{11} ions/s was typically observed during the measurements , another mechanism must be responsible for fluorine transport to the ionizer.

The presence of Cs, which was used as the work function lowering agent for testing the negative surface ionization concept, also aids in the transport of atomic F to the ionizer surface. Cs reacts spontaneously with AlF_3 to form CsF which has a higher vapor pressure than AlF_3. However,

CsF does not dissociate very efficiently at the ionizer temperature (1350°C) and typical operating pressure ($p \cong 2 \times 10^{-4}$ Torr) used during testing of the source for F^- generation. (According to thermodynamic calculations, the dissociation fraction of CsF at 1350°C and 2×10^{-4} Torr is ~ 0.86%) [25].) If we assume that the total Cs vapor flow equivalent is 13.3 μA (calculated from Eq. (12) for a Cs reservoir temperature of 200°C) and that 50% of the Cs vapor reacts to form CsF, then the ionization efficiency for F^- formation due to thermal dissociation of CsF is 52.3%. Based on these rough estimates, the efficiency for F^- formation is very high. However, more definitive measurements must be made before arriving at a final conclusion on this important issue.

9.0 Conclusions

The surface ionization source has proved to be a stable, reliable, versatile, and efficient means for generating beams of either highly electropositive or highly electronegative species without the requirement of ionizer interchange. This flexibility makes it a viable candidate for use in several research and applied science applications, including RIB generation. The source is also very simple and relatively inexpensive, which is important for RIB applications where contaminated sources that need repair must often be discarded. In addition, the source is designed so that parts can be easily cleaned and interchanged during routine maintenance. The highly permeable ionizer represents one of the principal achievements of these developments and is the first of its kind. Because of the high permeability characteristics of the ionizer, the probability of ionizing low-ionization-potential elements such as members the group IA elements during passage through the matrix is very high. Off-line testing of the source has demonstrated that it can be used to efficiently ionize feed materials such as Cs where measured ionization efficiencies exceeding 60% and space-charge-limited beams exceeding 18 μA have been realized. The source was found to be easy to operate in the negative ionization mode with no evidence of poisoning effects which plague more traditional negative surface ionization sources equipped with LaB_6 ionizers [11, 13]. Preliminary estimates suggest that this mode of operation is also quite efficient for highly electron negative species such as F. Based on estimates for vapor transport and thermal dissociation of CsF, the efficiency for F^- formation may exceed 50% for this mode of operation. However, because of the complexities introduced by the addition of Cs, the poor dissociation properties of the feed materials used in the testing of the source (AlF_3 and CsF), further studies must be made, perhaps with other work function lowering agents, such as Ba, Ce, or Eu, before a more definitive answer can be given to its efficiency for F^- generation. Research sponsored by the Oak Ridge National Laboratory , managed by Lockheed Martin Energy Research Corporation for the U.S. Department of Energy under contract number DE-AC05-96OR-22464.

References

[1] G. D. Alton, Nucl. Instr. and Meth. **B73**, 221 (1993).

[2] T. Bjørnstad, E. Hagebø, P. Hoff, E. Kugler, H. L. Ravn, S. Sundell, and B. Vosicki, Physica Scripta **34**:578 (1986).

[3] J. M. D'Auria, M. Dombsky, L. Buchmann, J. D. Vincent, and J. D, King, Nucl. Instr. and Meth. **B40/41** (1989) 418.

[4] N. Ikeda, Y. Shirakabe, J. Tanaka, T. Nomura, S. Ohkawa, S. Takieku, M. Oyaizu, H. Kawakami, and I. Katayama, Nucl. Instr. and Meth. **B70** (1992) 150.

[5] J. M. Lafferty, J. Appl. Phys, **22** 299 (1951).

[6] V. S. Fomenko, Emission Properties of Materials, JPRS-56579, (NTIS, U.S. Dept. Comm., Springfield, VA 1972).

[7] H. Ahmed and A. M. Broers, J. Appl. Phys, **43** 2185 (1972).

[8] S. Hosoki, S. Yamamoto, K. Hayakawa, and H. Okano, Jpn. J. Appl. Phys. Suppl. 2, Part 1, 285 (1974).

[9] H. Yamauchi, K. Takagi, I. Yuito and U. Kawabe, Appl. Phys. Lett. **29** (1976) 638.

[10] N. Kashihira, E. Vietzke, and G. Zellermann, Rev. Sci. Instr. **48**, 171 (1977).

[11] G. D. Alton, M. T. Johnson, and G. D. Mills, Nucl. Instr, and Meth. **A328** (1993) 154.

[12] B. Vosicki, T. Bjørnstad, L. C. Carraz, J. Heinemeyer, and H. L. Ravn, Nucl. Instr. and Meth. **186**, 307 (1981).

[13] A. A. Avidenko and M. D. Malev, Sov. Phys. Tech. Phys. **21** (1976) 1230.

[14] A Proposal for Physics with Exotic Beams at the Holifield Heavy Ion Research Facility, eds. J. D. Garrett and D. K. Olsen, Physics Division, ORNL, March 1991, unpublished.

[15] G. D. Alton, D. C. Haynes, G. D. Mills, and D. K. Olsen, Nucl. Instr, and Meth., **A328** (1993) 325.

[16] G. D. Alton, Particle Accelerators, **47** (1994) 133.

[17] The Chemical Vapor Deposition (CVD) of Ir on CBCF was performed by Ultramet, Inc., Pacoima, CA.

[18] I. Langmuir and K. Compton, Rev. Mod. Phys. **13** (1931) 191.

[19] "Space Charge Flow," P. R. Kirstein, G. D. Kino, and W. E. Waters, McGraw-Hill Book Company (1967), Appendix E, p. 495.

[20] PBGUNS, Thunderbird Simulation, Garland, Texas.

[21] G. D. Alton, Surf. Sci., **175**, 226 (1986).

[22] *The Kinetic Theory of Gases*, R. D. Present, McGraw-Hill Book Comapny (1958), Chap. 4, p. 63.

[23] H. Roβbach and B. Eichler, Zentralinstitut für Kernforschung, Rossendorf, Report ZfK-527 (1984).

[24] G. D. Alton and G. C. Blazey, Nucl. Instr. And Meth. **166** (1979) 105.

[25] Thermo-Calc is a thermodynamic -equilibrium phase diagram code developed by the Royal Institute of Technology, Stockholm, Sweden.

Table I. Low work function surface ionizers for negative ion generation.

Surface Material	Minimum Work Function
Ir/Re	3.7 eV
Ir/Cs	1.43 eV
Ir/Ce	2.33 eV
LaB_6	2.66 eV
LaB_6/Cs	2.06 eV
Ir/Eu	1.83 eV
Ir/Ba	2.08 eV
W/BaO/Rh/Os	1.5 eV
W/Ba	2.25 eV

Figure Captions

1. ORNL DWG 96M-7987. Schematic drawing of the self-extraction, spherical geometry, Positive (negative) surface ionization source equipped with a highly permeable Ir ionizer.

2. ORNL DWG 96M-7986. Scanning electron micrograph (SEM) of the highly permeable, Ir coated carbon-bonded-carbon-fiber (CBCF) ionizer with an intrinsic work function ϕ = 5.29 eV. CBCF density prior to coating: 0.25 g/cm^3; fiber diameter: ~ 6 μm. Ir coating thickness: ~ 5 μm.

3. ORNL DWG 95M-8398. Ion optics of the spherical geometry positive(negative) surface ionization source, shown schematically, in Fig. 1 as calculated by use of the computer code described in Ref. 20. The perveance, P_c, for the electrode geometry is $P_c = 8 \times 10^{-10}$ [A/V$^{3/2}$].

4. ORNL DWG 96M-7985. Work function ϕ versus relative coverage θ during adsorption of Cs on an Ir surface.

5. ORNL DWG 96M-7983. Relative coverage θ versus ionizer temperature for adsorption of Cs on an Ir surface ionizer as calculated by use of Eq. 11. The product of the change in entropy ΔS and temperature T from the gas phase to the adsorbed state is assumed to be ΔST = -0.4 eV.

6. ORNL DWG 96M-7308(B). Cs^+ ion current versus Cs oven temperature. Ionizer temperature: 1450°C; Extraction voltage: 600 V.

7. ORNL DWG 96M-7308(C). Cs^+ ion beam current versus ionizer temperature. Extraction voltage: 600 V; Cs oven temperature: 200°C.

8. ORNL DWG 96M-7308(A)R Cs^+ ion beam current versus extraction voltage. Perveance P_c for space charge limited flow of Cs^+: $P_c = 8x10^{-10}$ [A/V$^{3/2}$]. O: Cs oven temperature: 200°C; Δ: Cs temperature: 180°C; Ionizer temperature: 1450°C.

9. ORNL DWG 96M-7309(B). F^- ion beam current versus Cs oven temperature. Extraction voltage: –300 V; Ionizer temperature: 1350°C; Target reservoir temperature: 500°C; Feed material: AlF_3.

10. ORNL DWG 96M-7309(A)R. F^- ion beam current versus ionizer temperature. Cs oven temperature: 200°C; Extraction voltage: –300 V; Feed material: AlF_3.

11. ORNL DWG 96M-7309(F). F^- ion beam intensity versus extraction voltage. Cs oven temperature: 195°C; Ionizer temperature: 1350°C; Target temperature: 500°C; Feed material: AlF_3.

12. ORNL DWG 96M-7309(E). F^- ion beam current versus target reservoir temperature. Extraction voltage: –300 V; Ionizer temperature: 1350°C; Cs oven temperature: 200°C; Feed material: AlF_3.

13. ORNL DWG 96M-7309(D). Negative ion mass spectra of beams extracted from the positive(negative) surface ionization source, displayed in Fig. 1.

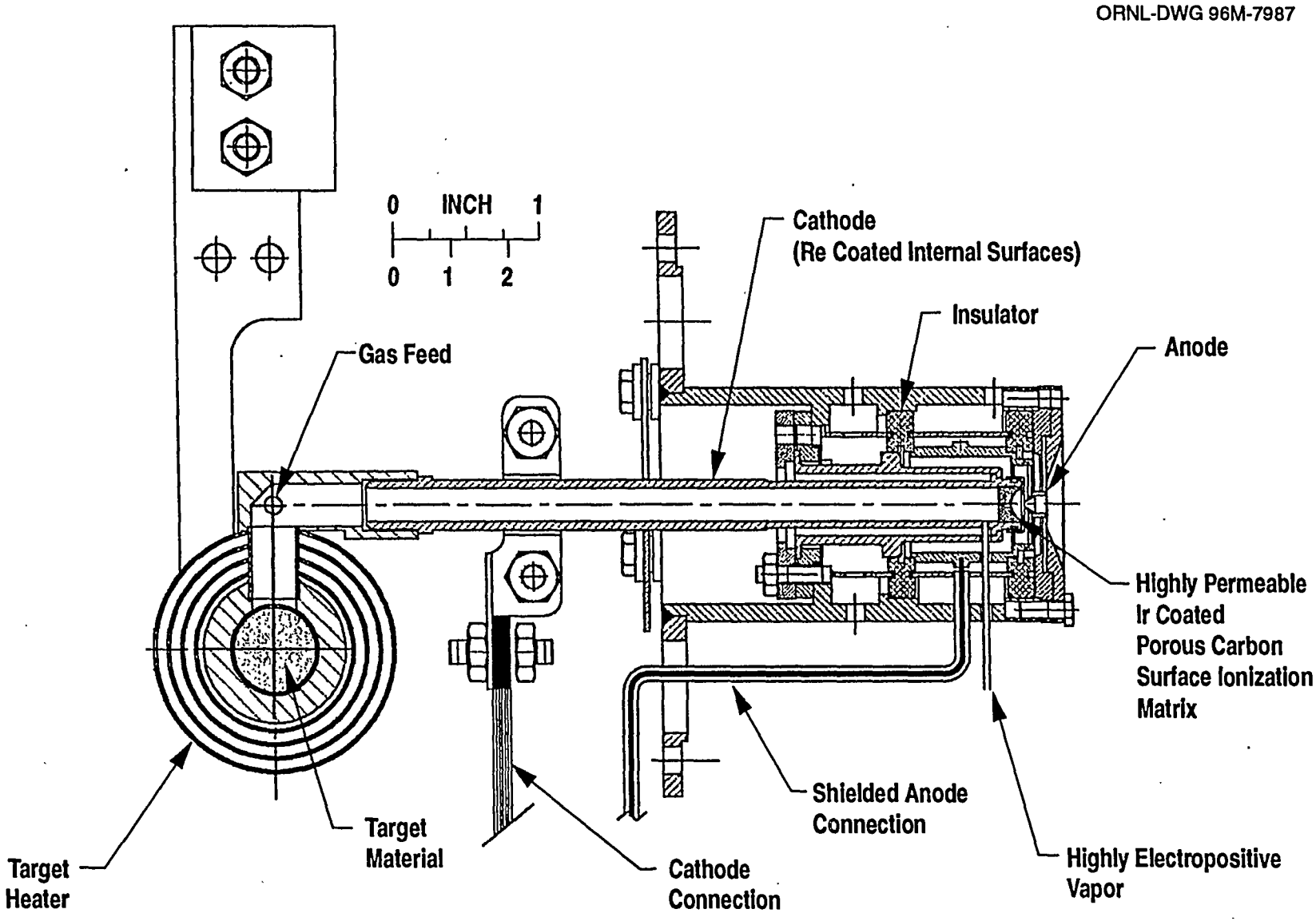
ORNL-DWG 96M-7987
0 INCH 1
0 1 2
Cathode
(Re Coated Internal Surfaces)
Insulator
Anode
Gas Feed
Highly Permeable
Ir Coated
Porous Carbon
Surface Ionization
Matrix
Target
Heater
Target
Material
Cathode
Connection
Shielded Anode
Connection
Highly Electropositive
Vapor

Fig.1

Ir Thickness: 1-2 microns
Work Function: 5.29 eV

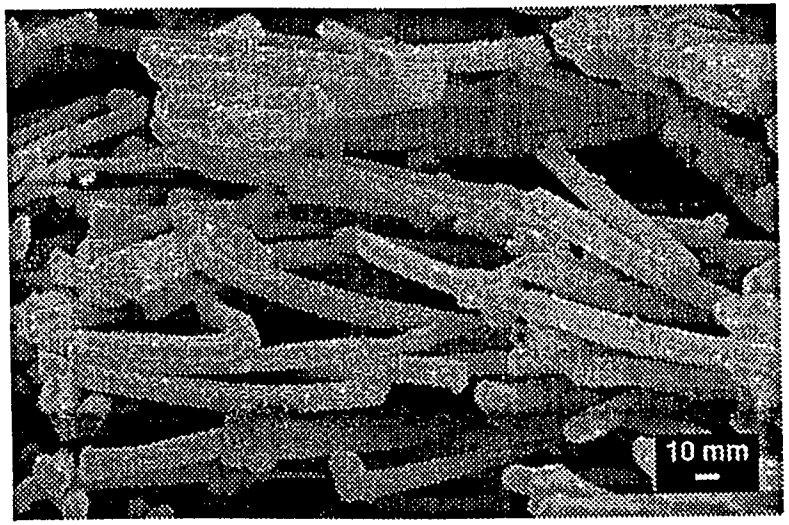

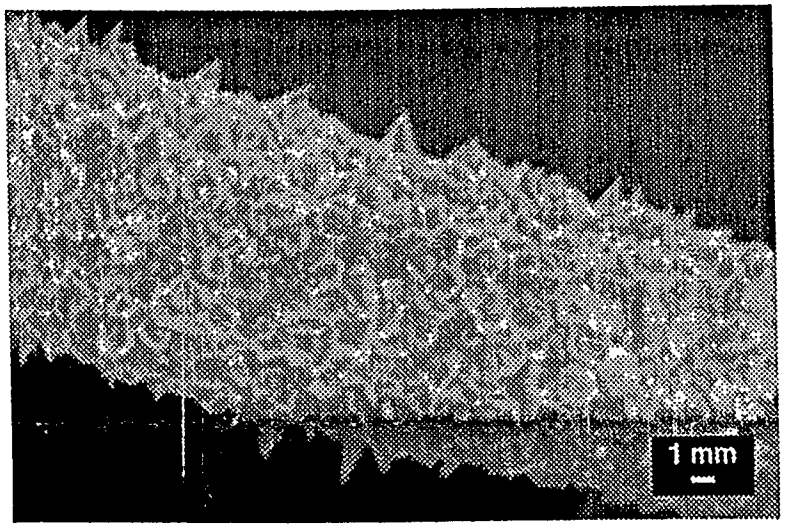

Fig. 2

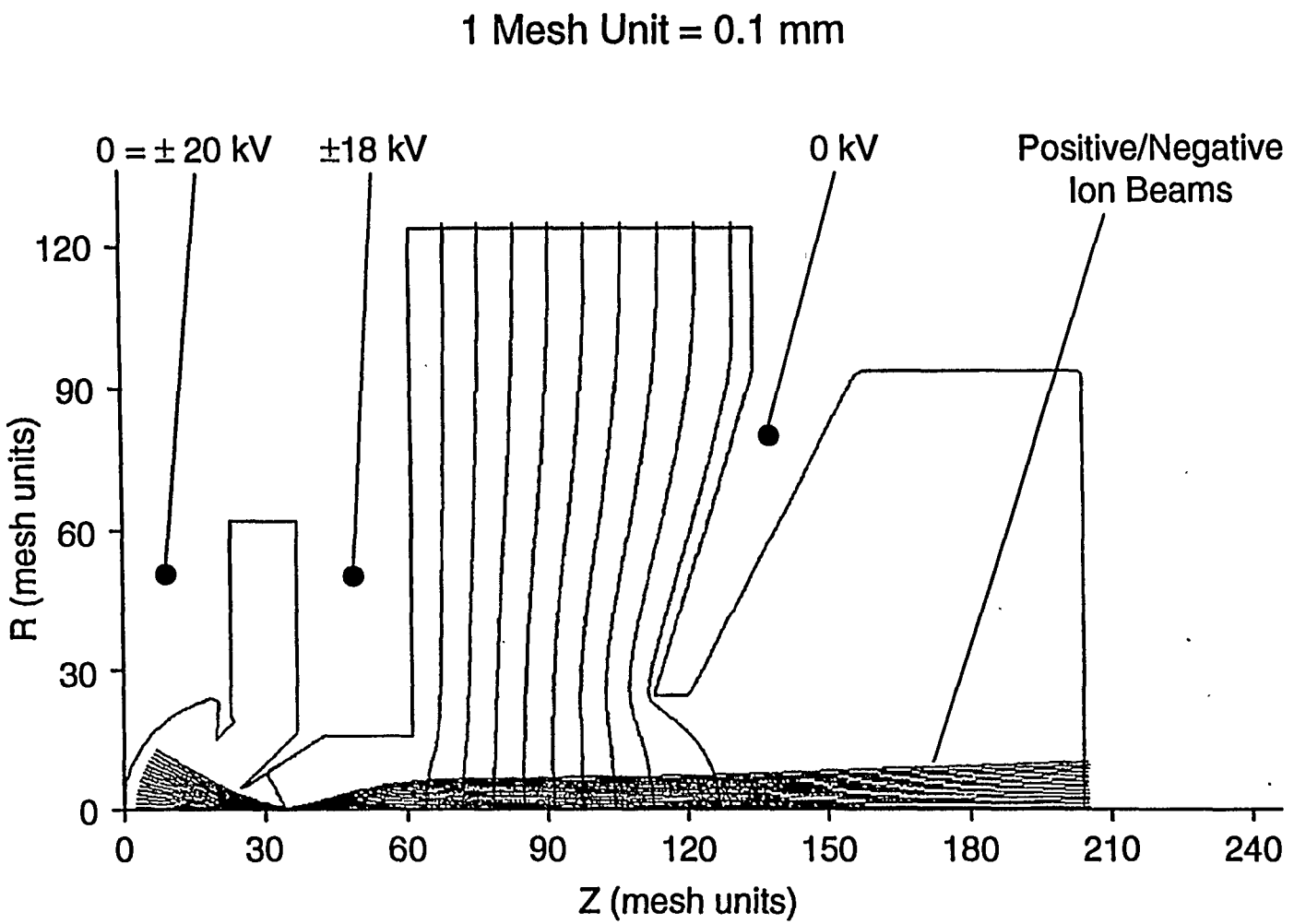
1 Mesh Unit = 0.1 mm
0 = ± 20 kV
±18 kV
0 kV
Positive/Negative
Ion Beams
R (mesh units)
0
30
60
90
120
0
30
60
90
120
150
180
210
240
Z (mesh units)

Fig. 3

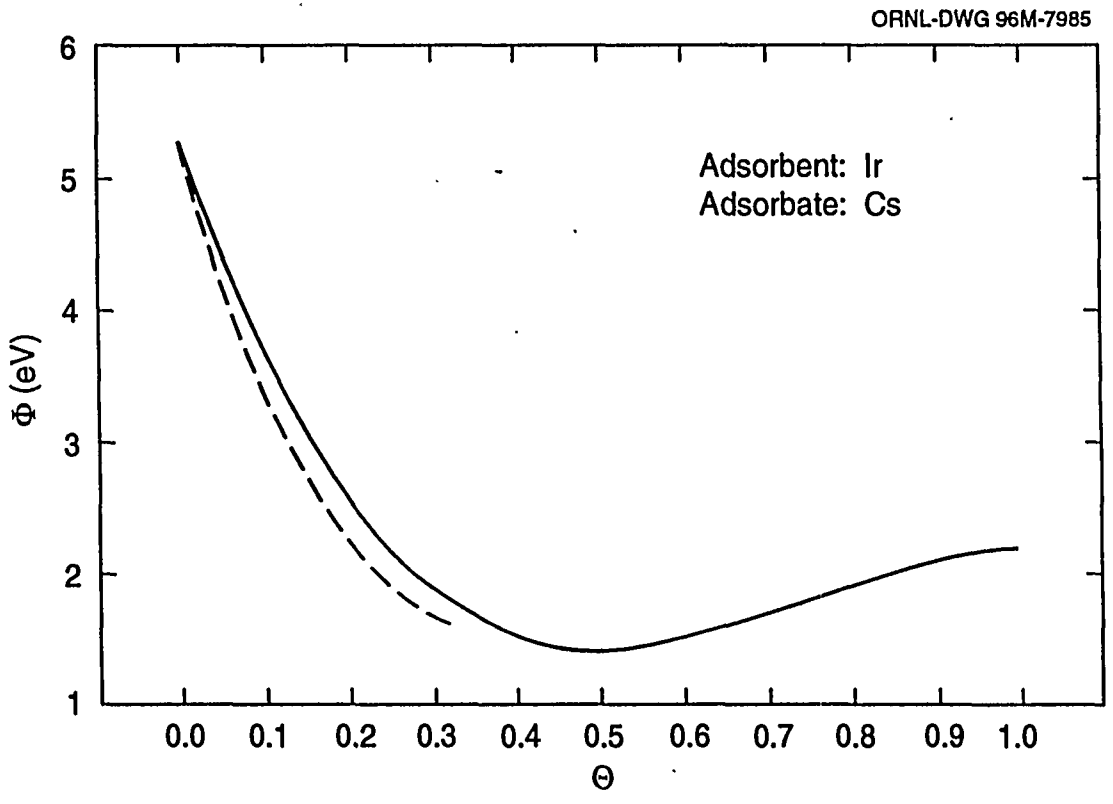
ORNL-DWG 96M-7985
Adsorbent: Ir
Adsorbate: Cs
Φ (eV)
Θ
6
5
4
3
2
1
0.0
0.1
0.2
0.3
0.4
0.5
0.6
0.7
0.8
0.9
1.0

Fig. 4

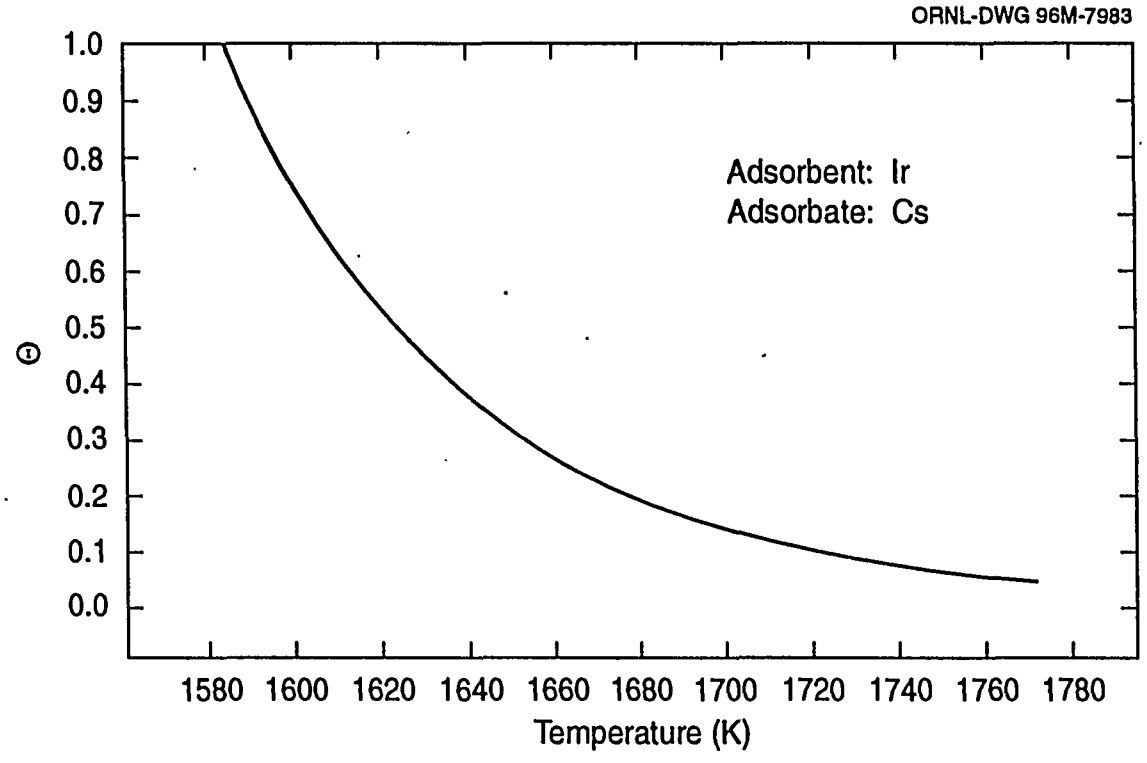
ORNL-DWG 96M-7983
1.0
0.9
0.8
0.7
0.6
0.5
0.4
0.3
0.2
0.1
0.0
Θ
Adsorbent: Ir
Adsorbate: Cs
1580 1600 1620 1640 1660 1680 1700 1720 1740 1760 1780
Temperature (K)

Fig. 5

ORNL-DWG 96M-7308(B)

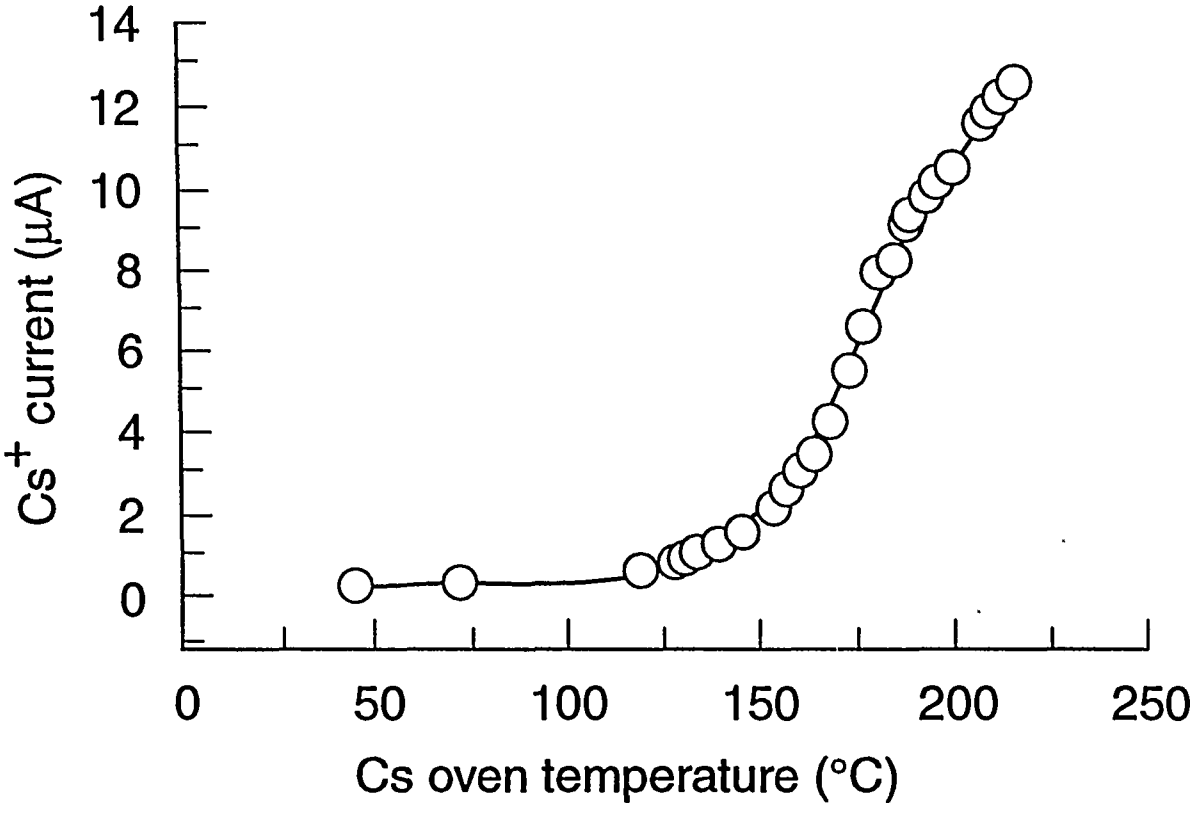

Fig. 6

ORNL-DWG 96M-7308(C)

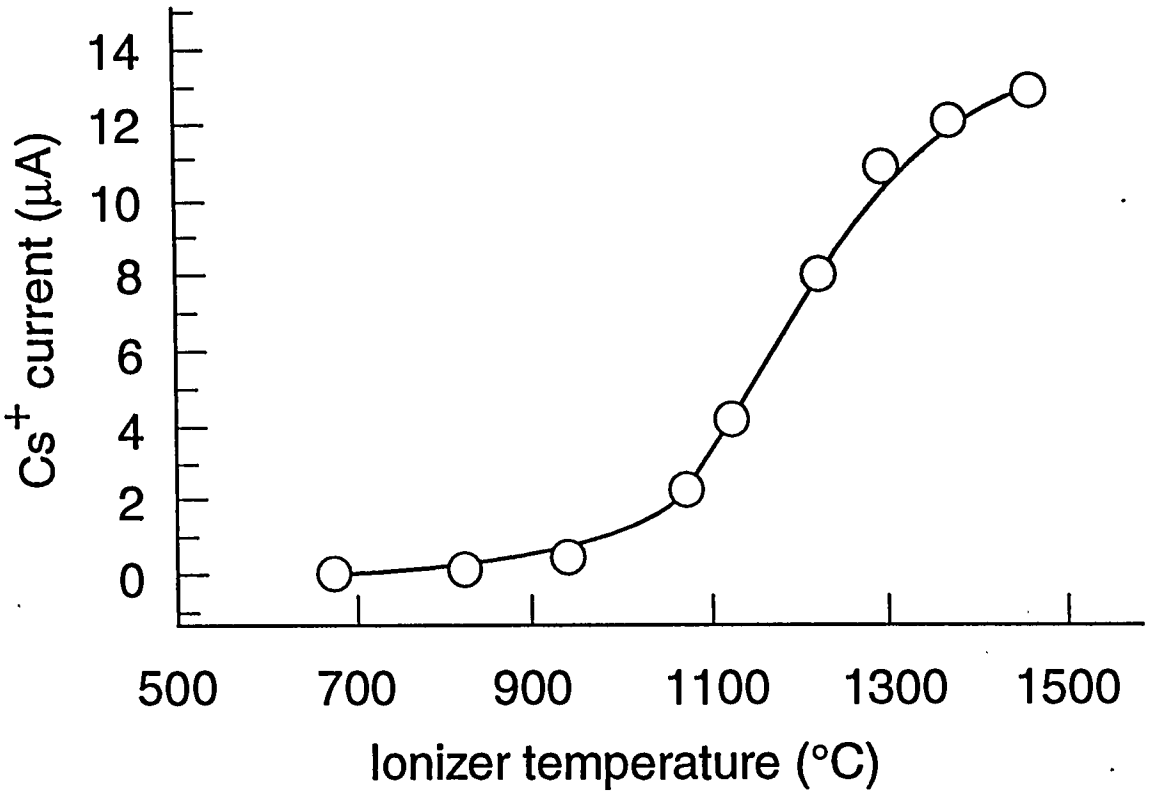

Fig. 7

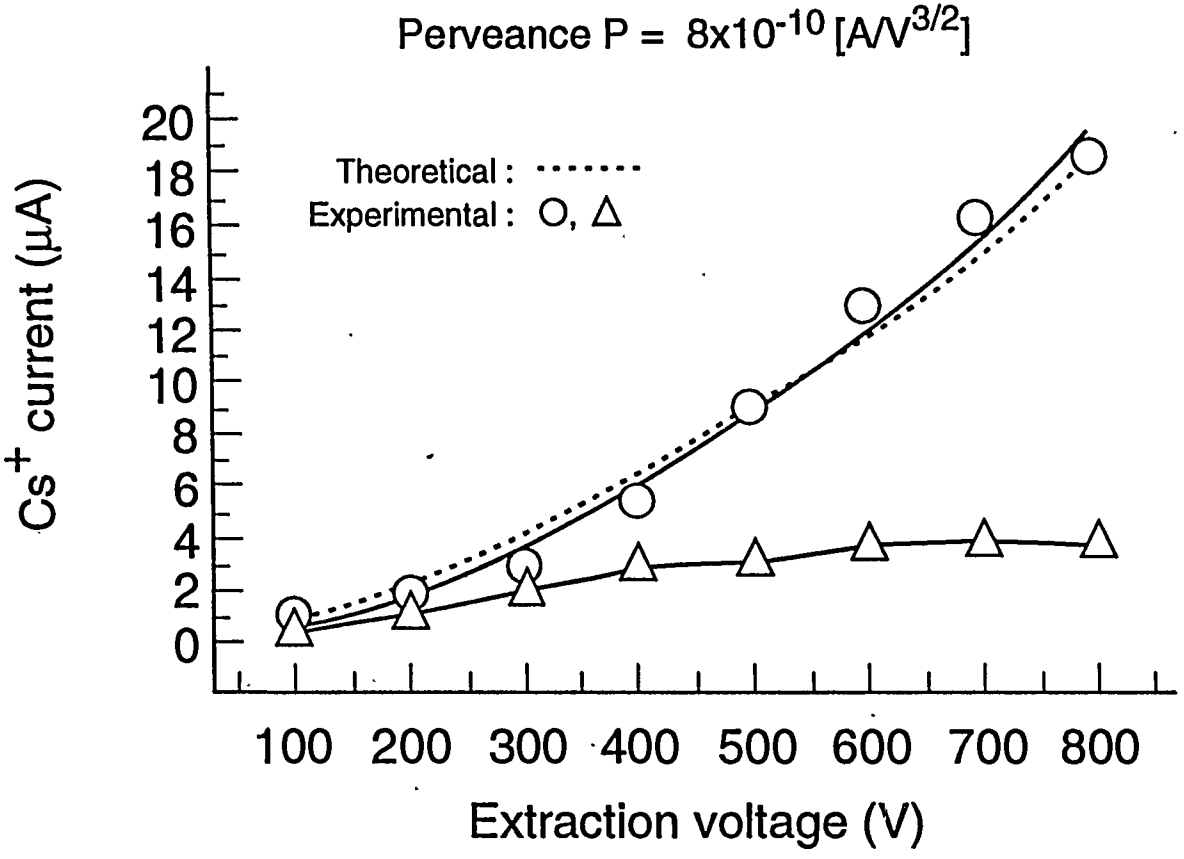
Perveance P = 8x10-10 [A/V3/2]
Theoretical : ·····
Experimental : O, Δ
Cs+ current (μA)
0
2
4
6
8
10
12
14
16
18
20
100 200 300 400 500 600 700 800
Extraction voltage (V)

Fig. 8

ORNL-DWG 96M-7309(B)

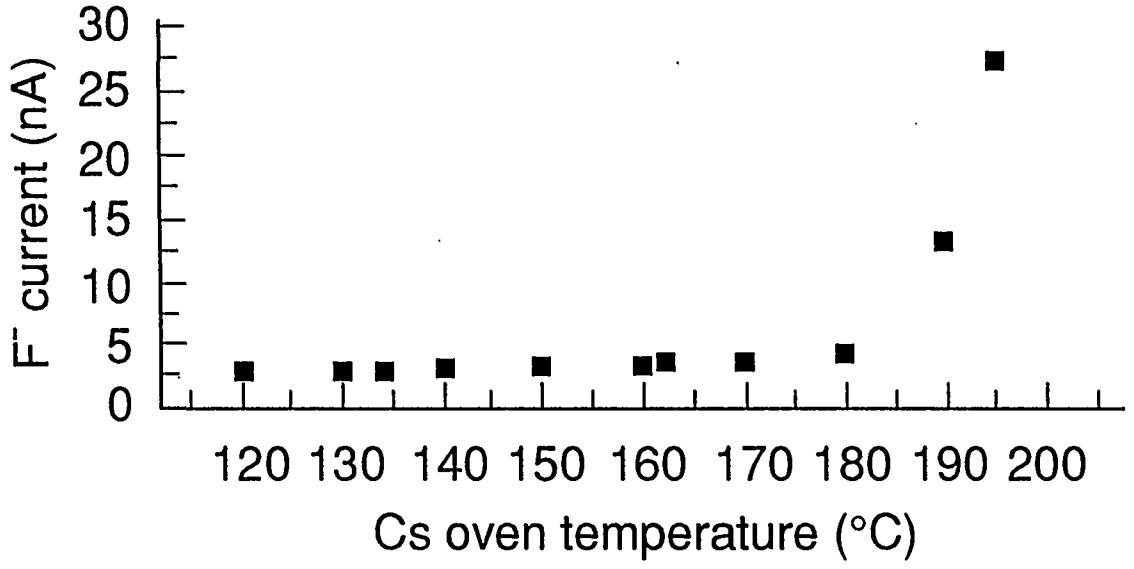

Fig. 9

ORNL-DWG 96M-7309(A)R2

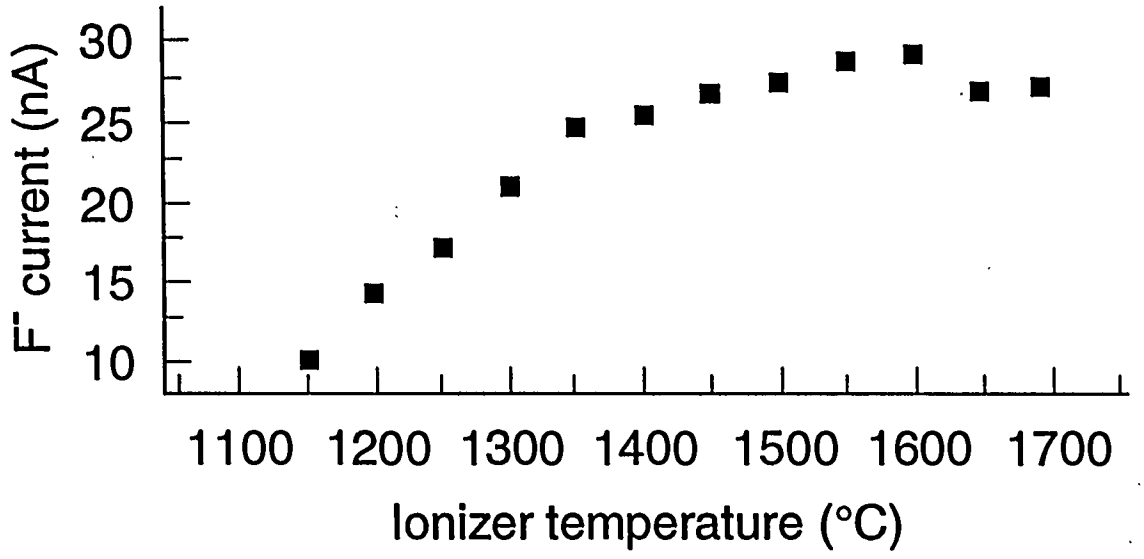

Fig.10

ORNL-DWG 96M-7309(F)

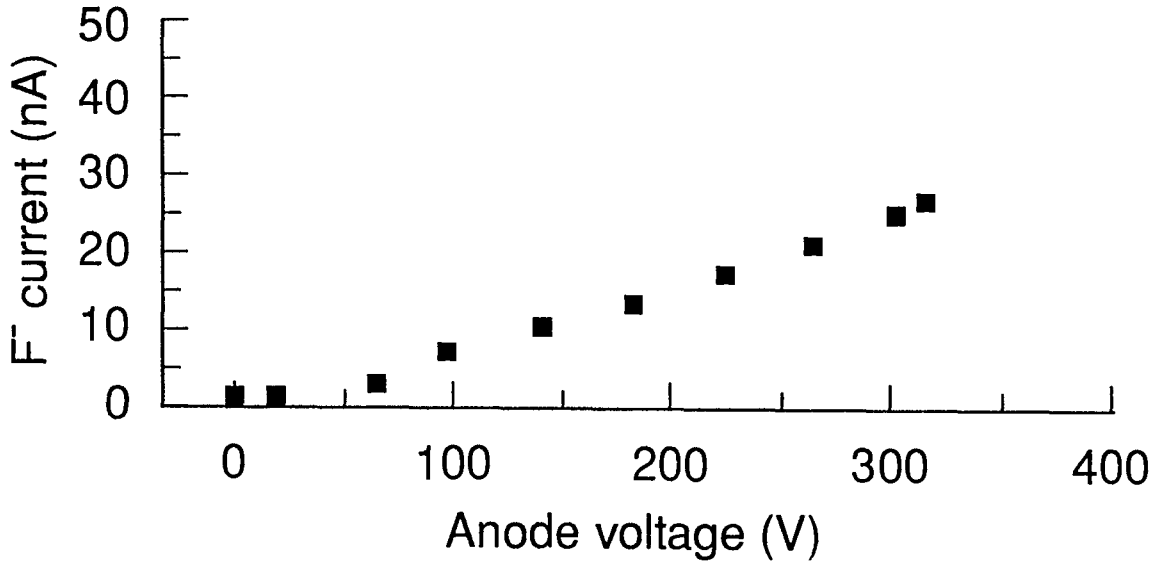

Fig. 11

ORNL-DWG 96M-7309(E)

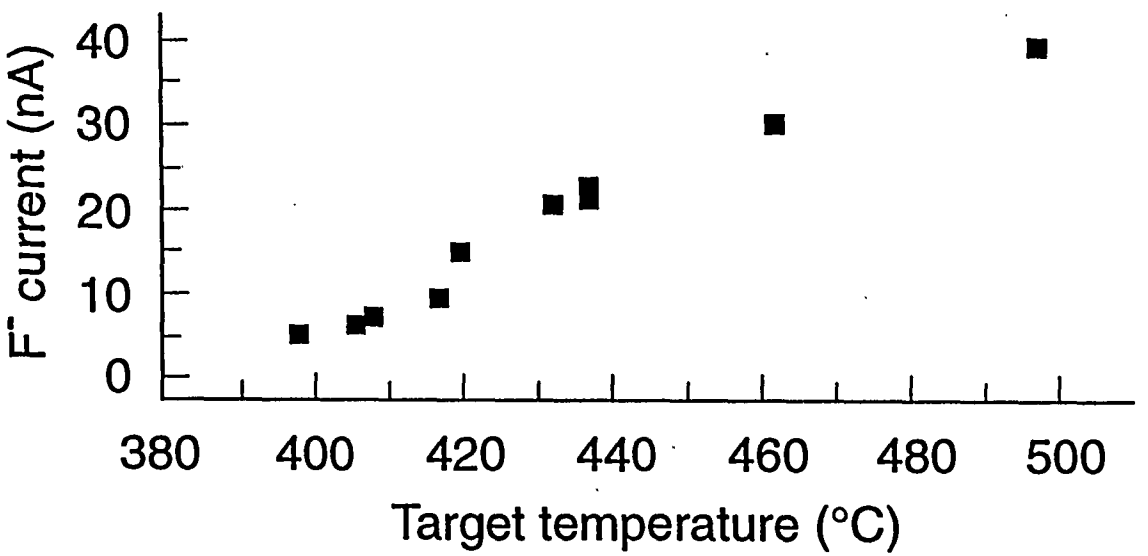

Fig. 12

ORNL-DWG 96M-7309(D)

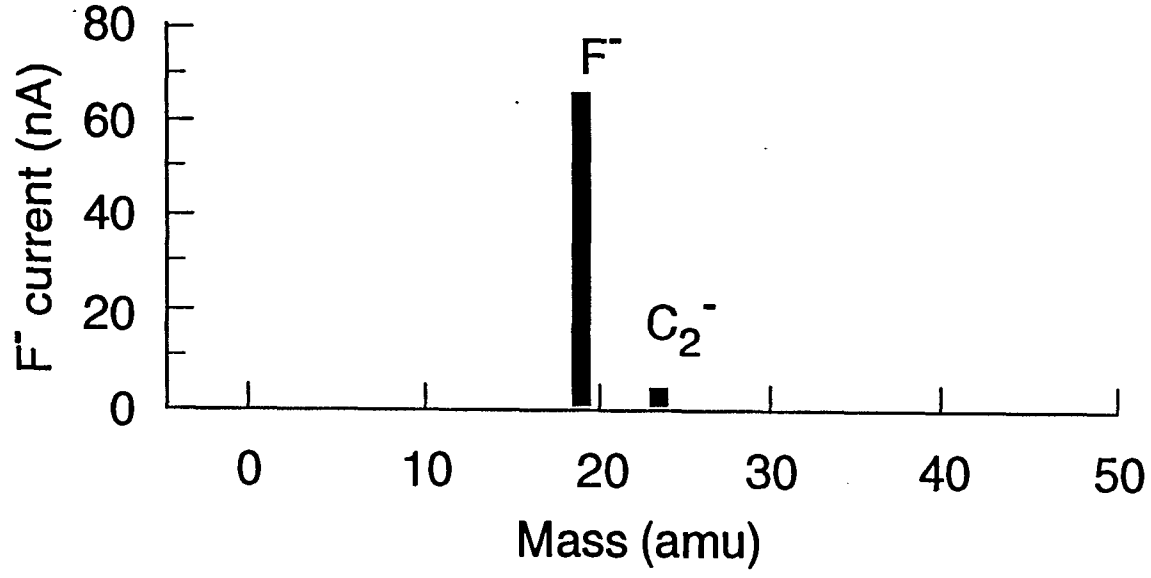

Fig. 13